J. Fluid Mech. (1996), *vol.* 318, *pp.* 223–236

Vaporization of a liquid drop suddenly exposed to a high-speed airstream

By D. D. JOSEPH, A. HUANG AND G. V. CANDLER
University of Minnesota, Minneapolis, MN 55455, USA

(Received 7 February 1995 and in revised form 5 September 1995)

Many studies of fragmentation of liquid drops at supersonic Mach numbers report the appearance of large amounts of mist. Photographs from other studies, which do not mention mist at all, strongly suggest that copious amounts of mist are formed at the earliest stages of fragmentation. In this paper, we present arguments and calculations which indicate that this mist is formed from condensed vapour arising from the flash vaporization of the hot and low-pressure liquid on the leeside of the drop. Low leeside pressures are produced by the rarefaction of the gas, the acceleration of the drop, and the high tensions generated by rapid stretching of the stripped liquid. The droplet temperature may rise because of heat transfer from the hot gas to thin drop filaments, and by viscous heating due to rapid deformation.

1. Introduction

The flash vaporization of liquid drops suddenly exposed to a high-speed airstream has not been considered in studies of aerodynamic breakup. In principle, by flash vaporization we mean the sudden reduction of a superheated liquid mass to vapour. In practice, we admit any mechanism which could lead to vapour in the short times in which the liquid drop is fragmented by high-speed air. There are many studies that mention the formation of copious amounts of mist (Reinecke & Waldman 1970; Waldman, Reinecke & Glenn 1972; Simpkins & Bales 1972) and still more that do not mention mist but speak of the formation of sprays (Ranger & Nicholls 1969; Yoshida & Takayama 1990). In an experiment, Engel (1958) showed that drops of millimetre diameter would be completely reduced to mist in the region between the detached shock and the surface of the drop at Mach numbers in the range of 1.3 to 1.7. She observed that the mist appeared to emanate from the leeward face of the water drop, while the remainder of the drop stayed essentially intact. She also pointed out that as the Mach number was increased, the mist formed sooner and in larger amounts, and as the water drop diameter was decreased, the mist also formed sooner. In a careful discussion of the most probable sources of the water mist, Engel rejected evaporation followed by condensation. Her arguments were based on the fact that evaporation takes much longer than the time elapsed before the appearance of the mist. However, she did not consider the mechanism of flash vaporization proposed here.

We have not found any literature which explicitly identifies flash vaporization as the cause of the mist coming off liquid drops behind a high-Mach-number shock wave. However, there are some studies of the flash vaporization of superheated water jets. Early investigations of the flash vaporization of superheated jets into still air at

atmospheric pressure were carried out by Schmidt (1949), Stephenson (1965), Fedoseev (1958), Brown (1960), Short (1962), and Ostrowski (1966). Brown (1960) reports that as the liquid temperature was increased, flashing and subsequent atomization of the liquid stream occurred over a fairly narrow temperature range. Gooderum & Bushnell (1969) did studies of very low-speed, low-Weber-number flashing jets of water into vacuum and monitored the drop sizes as a function of the temperature. Two different modes, namely 'flashing' and aerodynamic atomization, were considered.

Flash vaporization is associated with the condition where the ambient pressure is below the vapour pressure of the liquid. As is well known, very low pressures are generated at the back side of a spherical body moving forward at high speed in still air. The pressure at the front stagnation point is very high, but the pressure on the surface decreases rapidly to values which can be below the vapour pressure of the liquid. In the case of a liquid drop suddenly exposed to a high-speed airstream, the unsteady motion introduces an additional reduction of the pressure at the leeside of the drop due to its rapid acceleration by the air flow. This acceleration can be very large, and the resulting effect on the pressure is significant.

There are other effects that contribute to the reduction of the leeside pressure. The aerodynamic forces tend to strip off water from the equator of the drop. The stripping and stretching motions lead to the formation of water sheets or threads. The motion prevalent in these sheets or threads is extensional, which is associated with a pressure distribution that decreases in the flow direction. When this extensional motion is severe, the liquid may break in tension, which results in cavitation or vaporization of the liquid.

Behind the bow shock wave, the temperature increases dramatically. The deformation and the aerodynamic friction also promote an increase in the temperature of the drop. Because the time that it takes to form the mist is typically several hundred microseconds, it is unlikely that the drop's temperature would rise significantly. But even a modest temperature change would lead to a considerable increase of the vapour pressure, which would promote flash vaporization.

In the following, we present a detailed discussion of the aforementioned mechanisms which provide evidence for flash vaporization as the source of the mist produced after a liquid drop is struck by a high-speed airstream.

2. Pressure distribution on a sphere moving in still air

Flash vaporization may occur when the drop leeside pressure falls below the vapour pressure of the liquid. In this section we discuss the variation of the surface pressure with Mach number and Reynolds number for spheres moving at a constant supersonic speed. In reality, the drop deforms rapidly and accelerates, so these results are only directly applicable in the early stages of the aerodynamic dissemination process. However, we believe a knowledge of the steady pressure distribution provides some insights into the real problem. It should be noted that shock tube experiments show that the steady pressure distribution is established before the drop starts to deform.

Although the flow around a sphere at low speed has been carefully studied for many years, reports on supersonic flows are very few. Karyagin & Shvets' (1991) paper may be the best that we have found. Karyagin & Shvets did careful measurements of the pressure distribution around a sphere both in a 50 mm ballistic range equipped with a pressure channel and in a wind tunnel. Figure 1 is a cartoon representation of a shadowgraph from their work that shows a 4 cm diameter sphere at a free-stream Mach number of 2.8 and a Reynolds number of 2.8×10^8. This picture of the sphere

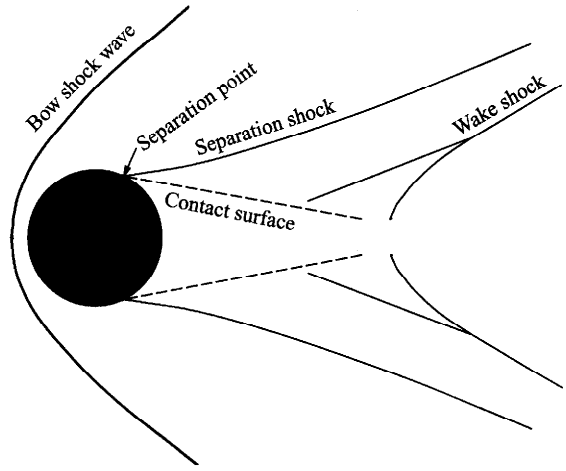

FIGURE 1. Cartoon representation of a shadowgraph of a sphere in supersonic flow, $M = 2.8$. From the experiment of Karyagin & Shvets (1991).

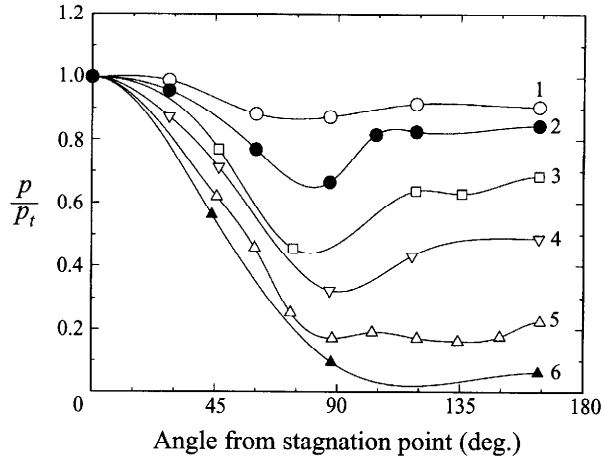

FIGURE 2. Experimental pressure distributions on spheres. Pressure is normalized by the stagnation point pressure, p_t; $M = 0.3$, 0.5, 0.7, 0.9, 1.2, 3.0, cases 1–6 respectively. (From Karyagin & Shvets 1991).

in free flight clearly shows the separation point, the detached bow shock, and the viscous wake.

The pressure distributions on the sphere measured by Karyagin & Shvets are shown in figure 2, where p_t is the stagnation-point pressure, which is related to the free-stream pressure p_∞ by the normal shock relation,

$$\frac{p_t}{p_\infty} = \left[\frac{2\gamma M^2 - (\gamma - 1)}{\gamma + 1}\right]^{-\gamma/\gamma-1} \left[\frac{(\gamma + 1)M^2}{2 + (\gamma - 1)M^2}\right]^{\gamma/\gamma-1} \left[1 + \frac{\gamma - 1}{2} M^2\right]^{\gamma/\gamma-1}, \qquad (2.1)$$

where γ is the ratio of specific heats of air and M is the free-stream Mach number relative to the sphere. Figure 2 shows that increasing the Mach number reduces the minimum pressure on the leeward surface of the sphere. For $M = 1.2$, the minimum p/p_t is about 0.25, and using (2.1) we get $p_{min}/p_\infty = 0.6$; for $M = 3.0$, the

minimum pressure relative to the free-stream pressure is $p_{min}/p_\infty = 0.5$. According to the experiments, the entire leeside has this pressure.

Experimental measurements of the pressure and temperature distribution on spheres in supersonic flow are not abundant. From the existing data we are not able to determine the details of the pressure and temperature on the sphere, in the wake, or in the recompression region. To understand these aspects of the problem better, we have used a computational fluid dynamics method to solve the Navier–Stokes equations for the steady supersonic flow of a perfect gas over a sphere. In these calculations, we are concerned with intermediate times during the interaction of the drop with the high-speed airstream. That is, we are considering times after the shock wave has passed over the drop, but before the drop has deformed significantly. This approach is valid based on the drop breakup times quoted by Engel and as a result of unsteady calculations that we have performed. We find that a steady flow is established during the time that it takes the flow to travel about two drop diameters. This is typically of the order of microseconds for millimetre-sized drops. The numerical method uses a finite-volume formulation with second-order upwind flux evaluations. The time-dependent equations are integrated in time using an implicit Gauss–Seidel line-relaxation method. We have performed grid convergence studies to ascertain that the 128×128 body-fitted grid is sufficiently fine. For more details of the numerical method, see Candler & MacCormack (1991).

We solved the compressible Navier–Stokes equations, supplemented by the perfect gas equation of state and the energy equation. We used a calorically perfect gas with a ratio of specific heats, γ, equal to 1.4. The viscosity dependence on the temperature is approximated with the Sutherland formula

$$\mu = \frac{c_0 T^{3/2}}{T + c_1}, \tag{2.2}$$

where $c_0 = 1.458 \times 10^{-5}\,\mathrm{P}$ and $c_1 = 110.3\,\mathrm{K}$ are constants, and T is the absolute temperature. The dilatational viscosity λ is related to μ by the Stokes assumption

$$\lambda = -\tfrac{2}{3}\mu. \tag{2.3}$$

A constant Prandtl number of 0.72 was used.

The boundary conditions are no slip at the drop surface, with a prescribed temperature that approximates the unknown temperature of the surface of the sphere. The incoming free-stream conditions are also fixed. The outflow is assumed to be supersonic, and the flow is axisymmetric.

We first reproduced cases 5 and 6 in figure 2. A comparison of the pressure distribution on the surface of the sphere with Karyagin & Shvets' experimental data is given in figure 3. The numerical results reproduce the experimental data except for a few minor differences. At $M = 1.2$, the computations show a slightly higher surface pressure for angles between 45° and 90°. And at $M = 3.0$, the recompression in the wake occurs slightly earlier than the experiment. However, the error bars on the experimental data are not known. Also, the surface temperature of the spheres used in the experiments is unknown.

It is interesting to note that the experimental data are insufficient to determine the minimum pressure on the surface for the case of $M = 3.0$. From the computational results, the minimum pressure on the surface in this case is found to be 15% of the free-stream pressure, whereas the experiment shows a minimum pressure ratio of 50%. The lower minimum pressure at $M = 3.0$ is a result of the flow staying attached farther around the sphere than for the $M = 1.2$ case. At this point, it is not clear

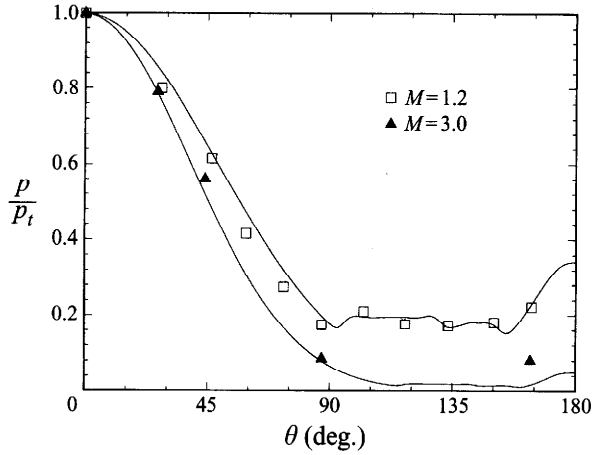

FIGURE 3. Comparison between experimental and numerical (curves) pressure distribution on a sphere with a diameter of 2.714 cm. In the computations, the sphere is assumed to have a temperature of 300 K, while the incoming airstream is at 250 K.

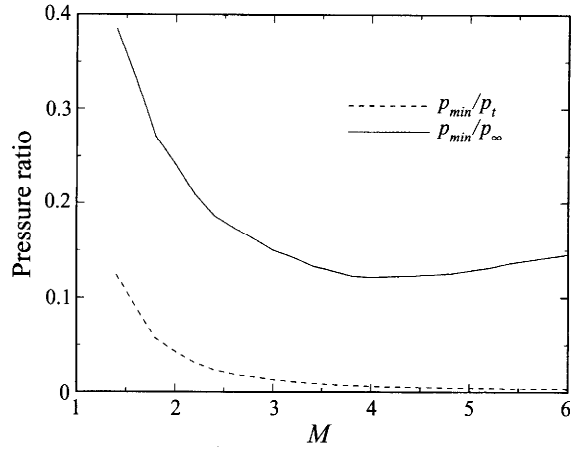

FIGURE 4. The minimum pressure on the surface of a sphere as a function of Mach number. p_∞ is the far-field pressure and p_t is the stagnation pressure.

whether the increased attachment length is a result of the higher Mach number or the higher Reynolds number for this case.

A clearer picture of how the minimum pressure changes with Mach number is given in figure 4. Here we plot the ratios of the minimum surface pressure to the free-stream pressure and to the stagnation-point pressure for a sphere of diameter 2.714 cm. Figure 4 shows that the ratio of the minimum pressure to the stagnation pressure decreases with increasing Mach number. However, since the stagnation pressure relative to the free-stream pressure increases with the square of the Mach number, the ratio of the minimum pressure to the free-stream pressure has a minimum of 0.12 at about $M = 4$. Hence, for usual free-stream pressures, the minimum pressure on the surface can be quite low. The variation of p_{min}/p_t with Mach number may be explained by the fact that the pressure on the leeside of a sphere is determined to a large extent by the location of the separation point. The separation point terminates

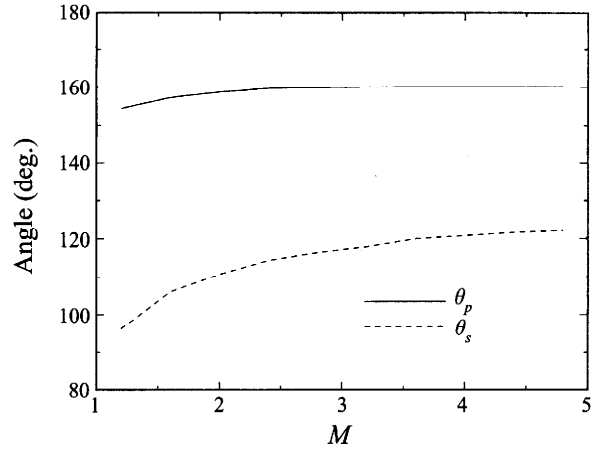

FIGURE 5. The location of the separation point, θ_s, and the minimum pressure point, θ_p, as a function of Mach number for the conditions used in figure 4. At high Mach number the separation point saturates at about 122°.

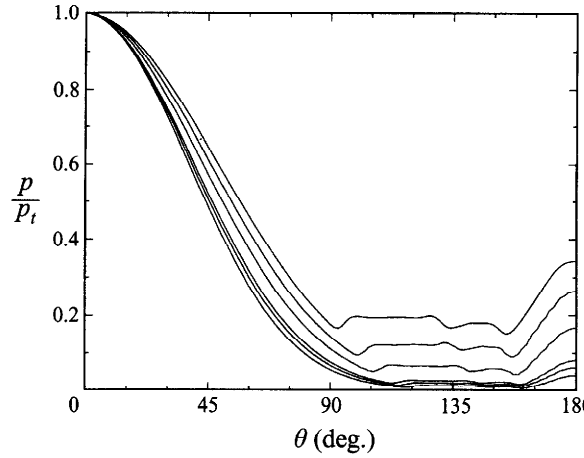

FIGURE 6. The computed pressure distributions on the surface of a sphere. From top to bottom, $M = 1.2$, 1.6, 2.0, 2.8, 3.2, 4.0. The first local pressure minimum corresponds to the separation point.

the expansion of the gas around the sphere. Thus, delayed separation allows the flow to expand to a lower pressure. This effect is evident in figure 5, which plots the angle of the separation point, θ_s, as a function of Mach number. We see that the location of separation increases with Mach number and gradually becomes constant at 122°. Also plotted in figure 5 is the location of the minimum surface pressure, θ_p. The minimum pressure is not located at the separation point, but always just before the pressure recovers. Thus, the pressure minimum is located nearer the rear centreline and varies less with Mach number than the separation location. This effect can be further illustrated by considering figure 6, which plots the surface pressure for Mach numbers between 1.2 and 4. There is a local minimum in the pressure at the separation point, then a fairly constant-pressure region in the recirculation zone, and then a further drop in the pressure to the minimum pressure. Then, the flow

recompresses near the sphere centreline. The surface pressure distribution becomes almost indistinguishable when the Mach number is greater than 4.

The relationship between the separation point and the minimum pressure is more obvious in figure 7, where pressure contours are displayed for three Mach numbers. We see that the pressure drops until the separation point, and then there is a region of more complicated pressure variation. Downstream of the separation point, the pressure near the surface is essentially constant. We also note that there is a region in the gas near the surface where the pressure becomes even lower than the minimum pressure on the surface.

We also computed cases with different sizes of spheres. The results are summarized in figure 8, which plots the ratio of the minimum surface pressure to the free-stream pressure as a function of Reynolds number for three different Mach numbers. Clearly, the minimum pressure decreases with Reynolds number, though this variation is fairly slow. Again, the smallest minimum pressure occurs for free-stream Mach numbers of about 4 for all Reynolds numbers that we simulated.

So far we have presented numerical results which indicate that the pressure is fairly low on the leeward side of a sphere travelling at high speed in still air. But since aerodynamic dissemination is an unsteady process, we need to turn our attention to the effect of acceleration of the drop on its pressure.

3. Pressure reduction by acceleration

Just as gravity causes hydrostatic pressure, a large acceleration may produce an extremely low pressure in a fluid, which may cause cavitation and vaporization (see Batchelor 1967). Let us consider the motion of a liquid drop in a high-speed airstream.

With respect to an inertial frame, the fluid within a liquid drop in unsteady motion satisfies the momentum equation

$$\rho\left(\frac{\partial \boldsymbol{V}}{\partial t} + \boldsymbol{V}\cdot\nabla\boldsymbol{V}\right) = -\nabla p + \mathrm{div}\cdot\boldsymbol{S} + \rho\boldsymbol{g} \tag{3.1}$$

where $\boldsymbol{S}$ is the extra stress due to deformation. We may divide the velocity into two parts

$$\boldsymbol{V} = U(t)\,\boldsymbol{e}_x + \boldsymbol{u} \tag{3.2}$$

where $U(t)$ is the time-varying speed of the drop mass centre, and $\boldsymbol{e}_x$ is the free-stream direction. Substituting (3.2) into (3.1), we get

$$\rho\left(\frac{\partial \boldsymbol{u}}{\partial t} + U\frac{\partial \boldsymbol{u}}{\partial x} + \boldsymbol{u}\cdot\nabla\boldsymbol{u}\right) = -\nabla p + \mathrm{div}\cdot\boldsymbol{S} + \rho\boldsymbol{g} - \rho\dot{U}\boldsymbol{e}_x, \tag{3.3}$$

which shows that the unsteady acceleration of the drop mass centre is like $\boldsymbol{g}$, and will generate an 'acceleration pressure'. If we put $\boldsymbol{u}$, $\boldsymbol{S}$, and $\boldsymbol{g}$ to zero, then $\mathrm{d}p/\mathrm{d}x = -\rho\dot{U} < 0$ so that the pressure, $p(x) = p(0) - \rho\dot{U}x$, decreases from the front of the drop to the back and is smallest at the leeside where mist is observed.

The simple mechanism just described applies to the drop as a whole using the velocity U of the centre of mass. An additional acceleration arises from the velocity $\boldsymbol{u}$ of deformations relative to the centre of mass. It would appear that the most important effects of this type are the extensional motions of streamers pulled out of the drop at early times when $\dot{U}$ is large and positive, and U is very small. To understand these effects better, we integrate (3.3) over the drop volume $\mathcal{V}$, assuming

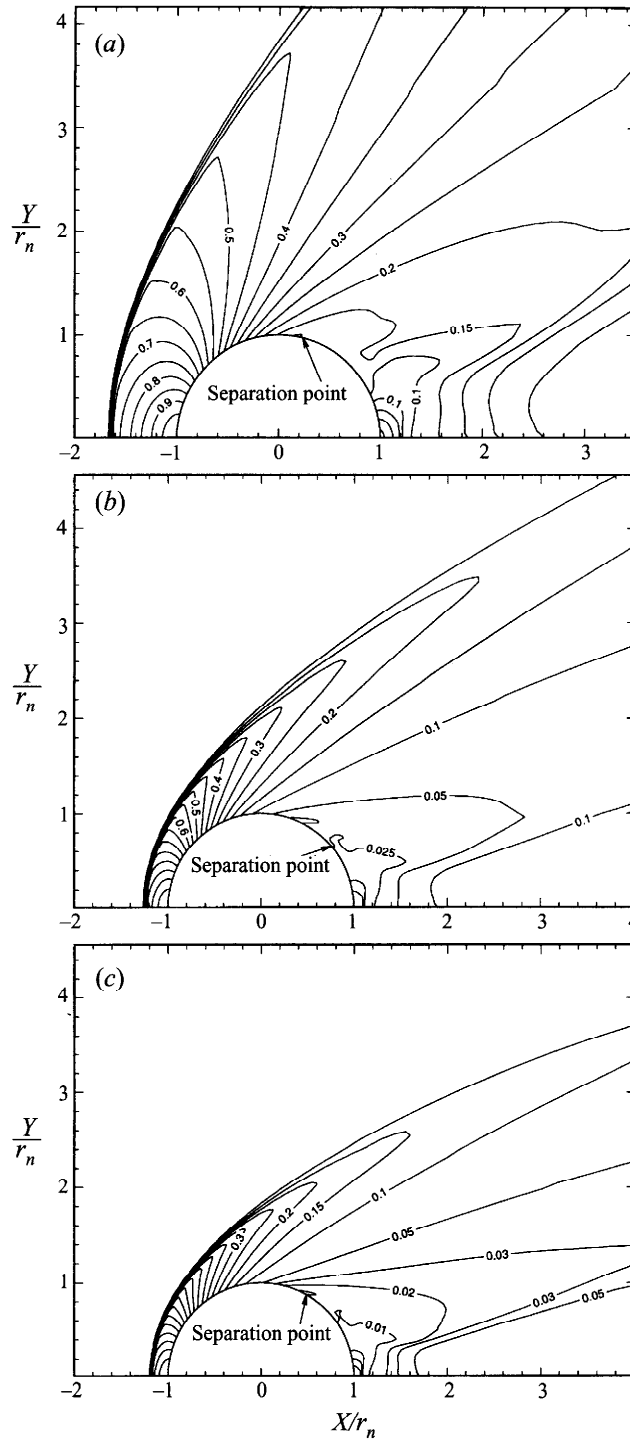

FIGURE 7. Pressure contours in the sphere flow field. Pressure is normalized by the stagnation point pressure, p_t. (*a*) $M = 1.6$; (*b*) $M = 2.8$; (*c*) $M = 4.0$.

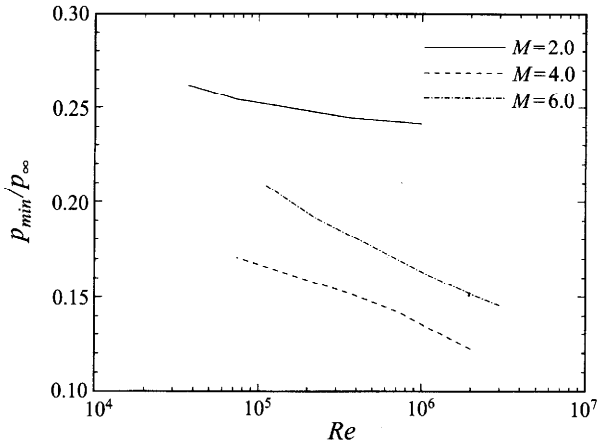

FIGURE 8. The minimum pressure on the surface of the sphere as a function of the Reynolds number based on the sphere diameter for three Mach numbers.

$\boldsymbol{g} = 0$, and obtain

$$\rho\Big(\int_\vartheta \frac{\partial \boldsymbol{u}}{\partial t}\,\mathrm{d}\vartheta + \dot{U}\,\vartheta \boldsymbol{e}_x + U\int_{\partial\vartheta}(\boldsymbol{e}_x\cdot\boldsymbol{n})\boldsymbol{u}\,\mathrm{d}s + \int_{\partial\vartheta}(\boldsymbol{u}\cdot\boldsymbol{n})\boldsymbol{u}\,\mathrm{d}s\Big) = -\int_{\partial\vartheta}(p\boldsymbol{n} - \boldsymbol{S}\cdot\boldsymbol{n})\,\mathrm{d}s. \quad (3.4)$$

The component of (7) in the free-stream direction is

$$\rho\Big(\int_\vartheta \frac{\partial u}{\partial t}\,\mathrm{d}\vartheta + \dot{U}\vartheta + U\int_{\partial\vartheta}(\boldsymbol{e}_x\cdot\boldsymbol{n})u\,\mathrm{d}s + \int_{\partial\vartheta}(\boldsymbol{u}\cdot\boldsymbol{n})u\,\mathrm{d}s\Big) = -\int_{\partial\vartheta}(p\boldsymbol{n} - \boldsymbol{S}\cdot\boldsymbol{n})\cdot\boldsymbol{e}_x\,\mathrm{d}s. \quad (3.5)$$

To get an estimate of the magnitude of the unknown terms, let us assume that the velocity field is purely extensional; we are thinking of streamers which are pulled out of the drop at early times in the drop breakup as in figure 9. Putting $x = 0$ at the base, we may imagine a purely extensional flow of the form

$$u = 2kx, \qquad v = -ky, \qquad w = -kz, \quad (3.6)$$

where k is the stretching rate. This flow model may represent the stripping and stretching stage of the drop deformation in a minimal way. However, an unrealistic feature of (3.6) is that it leads to a diagonal stress tensor with constant components when the stretching rate is independent of $\boldsymbol{x}$. For a Newtonian fluid of viscosity μ, $\boldsymbol{S}$ is given by

$$\boldsymbol{S} = \mu\begin{pmatrix} 2k & 0 & 0 \\ 0 & -k & 0 \\ 0 & 0 & -k \end{pmatrix}. \quad (3.7)$$

For this model, the streamwise equation of motion becomes

$$\rho(\dot{U} + 2kU)\vartheta + 2\rho(\dot{k} + 4k^2)A_\ell = -\int_{\partial\vartheta} p\boldsymbol{n}\cdot\boldsymbol{e}_x\,\mathrm{d}s, \quad (3.8)$$

where $A_\ell = \int_\vartheta x\,\mathrm{d}\vartheta$. The right-hand side of (3.8) is essentially the pressure difference across the drop and streamers in the direction of the flow and a large pressure difference leads to the low pressure favourable to vaporization on the leeside. The rate k of extension increases from zero, so that $\dot{k} > 0$ at times of interest.

The acceleration may be estimated using an appropriate drag coefficient. For a

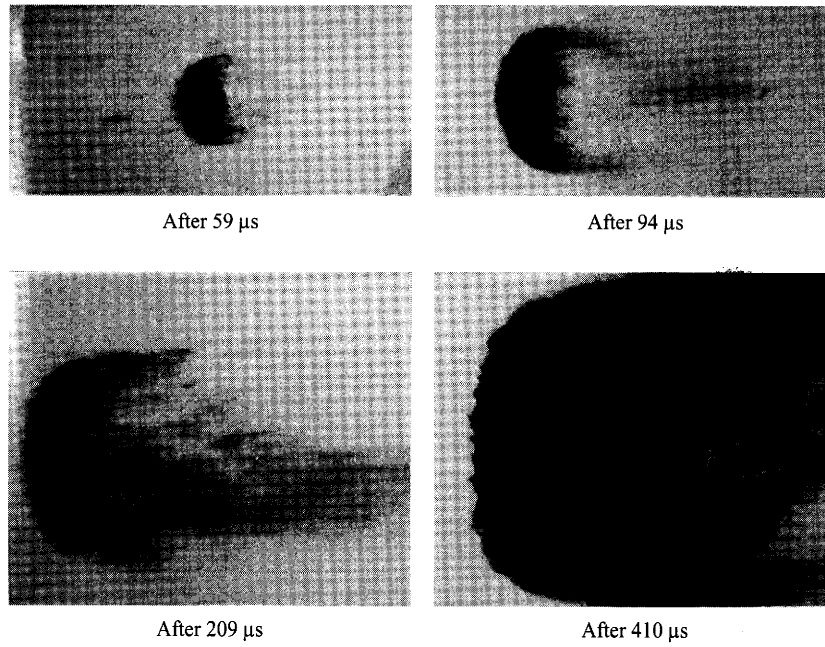

FIGURE 9. (From Engel 1958, figure 9) Shattering of a water drop in a shock tube; shock Mach number, M_s, is 1.5. Note the thin sheets and filaments torn from the drop at the drop equator.

sphere the drag coefficient, C_D, is defined as

$$C_D = \frac{D}{\frac{1}{2}\rho_a U_a^2 \pi R^2}, \tag{3.9}$$

where D is the drag, ρ_a and U_a are the density and speed of the air, and R is the drop radius. The sphere's equation of motion is:

$$\tfrac{4}{3}\pi R^3 \rho_w \dot{U} \simeq D = \tfrac{1}{2} C_D \rho_a U_a^2 \pi R^2, \tag{3.10}$$

where we have neglected the induced mass since $\rho_w \gg \rho_a$. Then, we can find the acceleration of the drop:

$$\dot{U} \simeq \frac{3 C_D \rho_a U_a^2}{8 \rho_w R}. \tag{3.11}$$

In one of Engel (1958)'s experiments, a drop with 0.135 cm radius was suddenly exposed to a Mach 1.5 airstream. If we take $C_D = 0.4$, and use Engel's flow conditions, we find

$$\dot{U} = 1.3 \times 10^6 \text{ cm s}^{-2}$$

from (3.11). This acceleration implies a drop velocity of 260 cm s^{-1} after 2×10^{-4} s of exposure to the airstream. Also from Engel's work we estimate an average k as roughly 2×10^3 s^{-1}. The right-hand side of (3.8) may be regarded as

$$-\int_{\partial \mathcal{V}} p \boldsymbol{n} \cdot \boldsymbol{e}_x \, \mathrm{d}s = \Delta p A, \tag{3.12}$$

where A is the drop cross-sectional area and Δp is the pressure difference across the drop. Then

$$\Delta p A \geqslant \rho(\dot{U} + 2kU)\mathcal{V} + 8\rho k^2 R \mathcal{V}, \tag{3.13}$$

where the inequality comes from the fact that $\dot{k} > 0$. If we approximate the drop volume as $A\ell$ where ℓ is the drop length which is seen to be about 0.54 cm at 2×10^{-4} s in Engel's experiment, we find that

$$\Delta p \simeq 3.1 \times 10^6 \text{ dyn cm}^{-2}. \tag{3.14}$$

This value is the same order as the stagnation pressure, so the pressure at the rear of the drop can be quite low, inducing flash vaporization or cavitation. Note that the acceleration that Engel (1958) inferred from the measurement of the drift speed of the drop for this case was even higher (6×10^6 cm s^{-2}) than the value used to get (3.14).

So far, we have separated the analysis of the drop surface pressure distribution into a steady and an unsteady part. We have shown that before a spherical drop deforms, it has a high stagnation pressure and low leeside pressure. This pressure distribution gives rise to a large acceleration which stretches the drop and causes a large pressure difference within the drop. Of course, the drop motion affects the flow of air over the drop; we have not considered this coupling. However, it is clear from our analysis that the drop leeside pressure is very low, which will cause flash vaporization.

We also note that in the simple extensional model we considered, we have neglected the viscous terms which produce additional stretching motion through shear forces. Thus, they tend to increase the tension in the drop and to further promote flash vaporization.

There is an additional mechanism that may produce vaporization due to the rapid stretching of the liquid during aerodynamic dissemination.

4. Vaporization in a flowing liquid

For a liquid in motion, the stress $\boldsymbol{T}$ is given by

$$\boldsymbol{T} = -p\mathbf{1} + \boldsymbol{S}, \tag{4.1}$$

where $\boldsymbol{S}$ is again the extra stress due to motion. Here p is chosen to satisfy the constraint of incompressibility, and is not determined by a constitutive relation or an equation of state.

Now, the question arises as to how to determine the cavitation threshold in a flowing liquid. When the liquid is at rest or moving slowly, the cavitation threshold is simply

$$p < p_s, \tag{4.2}$$

where p_s is the vapour pressure of the liquid, which is usually a function of temperature. However, in a flowing liquid the liquid does not understand the decomposition of the stress into $p\mathbf{1}$ and $\boldsymbol{S}$, and the cavitation threshold (4.2) is meaningless. Rather, we must consider the state of stress at every point.

This requires that we compare the components on the diagonal of $\boldsymbol{T}$ in a coordinate system in which $\boldsymbol{T}$ is diagonal. In such a coordinate system, suppose that

$$\mathscr{T}_{11} \geqslant \mathscr{T}_{22} \geqslant \mathscr{T}_{33}. \tag{4.3}$$

Different rupture criteria involving the three principal stresses can be proposed and tested in experiments. An attractive possibility is that the liquid will break (cavitate) at a point if

$$\mathscr{T}_{11} \geqslant \mathscr{T}_m, \tag{4.4}$$

where $\mathscr{T}_m$ is the breaking threshold. Now, we can relate this breaking threshold to

the cavitation threshold through $\mathscr{T}_m = -p_s$. Then, we should see vapour whenever and wherever

$$\mathscr{T}_{11} \geqslant -p_s. \tag{4.5}$$

This criterion is a generalization of the cavitation threshold (4.2), and may be related to a Newtonian fluid in motion for which

$$\mathscr{T}_{11} = -p + 2\mu \frac{\partial u}{\partial x}. \tag{4.6}$$

Then, we can expect the formation of vapour where the rate of stretching

$$\dot{s} = \frac{\partial u}{\partial x} \tag{4.7}$$

is large enough that

$$\dot{s} \geqslant \frac{p - p_s}{2\mu}. \tag{4.8}$$

In practical applications, p_s can be replaced with an empirical cavitation pressure, say $\tilde{p}_s$, which is an outgassing criterion associated with the presence of impurities. For more about the cavitation criterion for a flowing liquid, see Joseph (1994).

During aerodynamic dissemination, the stretching rates $\dot{s}$ of threads stripped from the equator of a drop can be huge. Thus, the liquid in the threads may flash into vapour.

5. Aerodynamic and viscous heating of the drop

Because the vapour pressure increases with the drop temperature, it is important to consider mechanisms for the heating of the drop. There are two primary causes of drop heating: aerodynamic heating and frictional heating due to rapid drop deformation.

For high-Mach-number flows, Tauber & Menees (1986) obtained an expression for the stagnation point heat transfer rate for a sphere (in W cm^{-2}):

$$q \simeq 5.79 \times 10^{-12} \left(\frac{\rho_a}{R}\right)^{1/2} U_a^3 \left(1 - \frac{h_w}{h_o}\right), \tag{5.1}$$

where ρ_a and U_a are the free-stream density and speed in g cm^{-3} and cm s^{-1} respectively. R is the drop radius in cm, and h_w and h_o are the wall and total enthalpies respectively.

For example, a 2 mm diameter drop travelling at Mach 3 in ambient air has a stagnation heat transfer rate of about 300 W cm^{-2}. This is a substantial heat transfer rate, but it only acts during the drop breakup time, which is typically several hundred microseconds. Therefore, because the thermal diffusivity of typical drop liquids is very small, only a thin layer of the drop is heated before the drop is destroyed. For a water drop at the above conditions, a time-dependent heat transfer analysis shows that at the stagnation point of the drop the temperature rises only 11 K during 200 μs. The thermal layer is about 5% of the drop radius. Therefore, the convective heating of the drop by the surrounding air is insignificant.

However, the heating of sheets of liquid stripped away from the drop can be important since the ratio of the surface exposed to hot gas to the volume of liquid to

be heated is then large (see figure 9). We may model this by an initial value problem for the heating of a liquid sheet of thickness ℓ:

$$\rho C_p T_t = \kappa T_{yy}, \qquad T(y,t) = T_w \quad \text{at} \quad y = 0, \ell, \quad T(y,0) = T_o, \tag{5.2}$$

where the surface temperature, T_w, is greater than the initial temperature, T_o, of the strip. The solution of this problem can be expressed as

$$T - T_w = \sum_{n=1} \theta_n(0)\, \mathrm{e}^{-n^2\pi^2\tau} \sin n\pi y, \quad \theta_n(0) = \tfrac{1}{2} \int_0^{\ell} \theta_0(y) \sin n\pi y \, \mathrm{d}y$$

where $0 \leqslant y \leqslant 1$ is made dimensionless with the strip thickness ℓ, $\tau = t\kappa/\rho C_p \ell^2$ is the dimensionless time, $\alpha = \kappa/\rho C_p$ is the thermal diffusivity, and $\theta_o = T_o - T_w$. Taking $\ell = 10^{-2}$ cm as the thickness of the thermal layer calculated in the previous paragraph and putting $\alpha = 6.2 \times 10^{-4}\,\mathrm{cm}^2\, s^{-1}$ for an organic liquid, we find that $\tau = 3.1 \times 10^{-3}$ after 500 μs. Then $\mathrm{e}^{-\pi^2\tau} = 0.97$ so we get fairly rapid heating of our initially cold strip. When the ambient air temperature is very high, as behind a bow shock at high M, a rise of the temperature of liquid stripped from the drop equal to 3% of the difference between the drop and air temperature is substantial and could lead to flash vaporization.

Photographs by Engel (1958) and others of the breakup of liquid drops in high-Mach-number streams show that very violent deformations occur over small times. The rapid deformations give rise to potentially large frictional heating accompanied by a significant temperature rise. The heating is associated with the term $2\mu \boldsymbol{D} : \boldsymbol{D}$ in the energy equation of the liquid, where $\boldsymbol{D}$ is the deformation gradient. This term may be large around the equator of the drop where the strong shearing action of the air rapidly stretches the liquid. Also, as the drop is flattened by the strong streamwise pressure gradient, significant frictional heating may occur. Both of the processes are very complicated, and require further detailed analysis to determine their relative importance. However, it is clear that the frictional heating points in the direction of rising temperature and vapour pressure, making flash vaporization more likely.

6. Conclusion

We identified five sources of low pressure and high temperature at the leeside of liquid drops in supersonic and hypersonic flow. These five sources are: (i) the rarefaction of the gas as it passes over the sphere in steady flow, (ii) the low pressure at the leeside produced by acceleration of the drop, (iii) the high tensions equivalent to low pressures produced by extensional motions of matter stripped from the drop, (iv) the frictional heating which is inevitable for the huge strains required for drop breakup, and (v) the heating of sheets and filaments torn from the drop by hot air. The steady flow problem was solved exactly by numerical simulation and the other mechanisms were discussed in a heuristic way. The conditions for flash vaporization arise at very early times; in milliseconds these severe conditions have relaxed and vaporized gas could recondense and evaporate in a normal way.

We would like to acknowledge support from the Army Research Office, the ERDEC, the National Science Foundation, and the Department of Energy. Computer time was provided by the University of Minnesota Supercomputer Institute.

REFERENCES

BATCHELOR, G. K. 1967 *An Introduction to Fluid Dynamics*, chap. 6. Cambridge University Press.

BROWN, R. 1960 Sprays formed by flashing liquid jets. PhD Dissertation, University of Michigan, Ann Arbor.

CANDLER, G. V. & MACCORMACK, R. W. 1991 The computation of hypersonic ionized flows in chemical and thermal nonequilibrium. *J. Thermophys. Heat Transfer* **5**, 266–273.

ENGEL, O. G. 1958 Fragmentation of waterdrops in the zone behind an air shock. *J. Res. Natl Bur. Stand.* **60**, 245–280.

FEDOSEEV, V. A. 1958 Dispersion of a stream of superheated liquid. *Colloid J.* **20**, 463–466.

GOODERUM, P. & BUSHNELL, D. 1969 Measurement of mean drop sizes for sprays from superheated waterjets. *J. Spacecraft Rockets* **6**, 197–198.

JOSEPH, D. D. 1995 Cavitation in a flowing liquid. *Phys. Rev.* E **51**, R1649–R1650.

KARYAGIN, V. P. & SHVETS, A. I. 1991 Experimental investigation of the separation of flow around a sphere. *Izv. Akad. Nauk SSSR* No. 1, 152–156.

OSTROWSKI, H. S. 1966 Evaporation and induced air flows in sprays produced by superheated water jets. PhD Dissertation, University of Michigan, Ann Arbor.

RANGER, A. A. & NICHOLLS, J. A. 1969 Aerodynamic shattering of liquid drops. *AIAA J.* **7**, 285–290.

REINECKE, W. G. & WALDMAN, G. D. 1970 A study of drop breakup behind strong shocks with applications to flight. *SAMSO-TR*-70-142, Avco Systems Division.

SCHMIDT, J. M. 1949 An experimental study of the behavior of liquid streams injected into a low-pressure chamber. *Jet Propulsion Lab., California Institute of Technology.*

SHORT, W. L. 1962 Some properties of sprays formed by the disintegration of a superheated liquid jet. PhD Dissertation, University of Michigan, Ann Arbor.

SIMPKINS, P. G. & BALES, E. L. 1972 Water-drop response to sudden accelerations. *J. Fluid Mech.* **55**, 629–639.

STEPHENSON, J. M. 1965 A study of cavitation and flashing flows. *Washington State Institute of Technology Bull.* 290.

TAUBER, M. E. & MENEES, G. P. 1986 Aerothermodynamics of transatmospheric vehicles. *AIAA Paper* 86-1257.

WALDMAN, G. D., REINECKE, W. G. & GLENN, D. 1972 Raindrop breakup in the shock layer of a high-speed vehicle. *AIAA J.* **10**, 1200–1204.

YOSHIDA, T. & TAKAYAMA, K. 1990 Interaction of liquid droplets with planar shock waves. *Trans. ASME J. Fluids Engng* **112**, 481–486.